JOURNAL OF APPLIED ELECTROCHEMISTRY 25 (1995) 823–832

An electrochemical study of reduced ilmenite carbon paste electrodes

Y. MARINOVICH, S. BAILEY

A. J. Parker Cooperative Research Centre for Hydrometallurgy, School of Applied Chemistry, Curtin University of Technology, Bentley 6102, Western Australia

J. AVRAAMIDES, S. JAYASEKERA

A. J. Parker Cooperative Research Centre for Hydrometallurgy, Mineral Processing Laboratory, Waterford, 6152, Western Australia

Received 25 August 1994; revised 16 January 1995

The anodic dissolution of reduced ilmenite has been studied using the carbon paste electrode technique. To understand the polarization behaviour of reduced ilmenite, the polarization behaviour of iron oxide and iron powder carbon paste electrodes has also been investigated. It was shown that synthetic rutile and reduced ilmenite promoted the anodic dissolution of iron.

1. Introduction

Reduced ilmenite (RI) is an intermediate product of the Becher process [1, 2], which is used to upgrade ilmenite (~60% TiO_2) to synthetic rutile (SR) (92–95% TiO_2). RI is produced by heating ilmenite with coal at about 1100 °C; this reduces the iron content to metal. The metallic iron is honeycombed within a matrix of TiO_2. The iron is removed from RI by corrosion with oxygen in a 0.5–1.6% w/v aqueous ammonium chloride solution. The finely divided iron oxide and coarser synthetic rutile products can be separated by counter current washing.

It was shown [3] that the reaction between oxygen and iron in reduced ilmenite was diffusion controlled and that ammonium chloride plays a special role in the corrosion reaction in a number of ways. First, by acting as a buffer, thus preventing local high pH values forming near the iron surface (from the oxygen reduction reaction) which would cause the precipitation of iron oxide within the grain. Secondly, ammonia formed at high pH increases the solubility of Fe^{2+}, probably by forming a ferrous-ammonia complex.

RI is a unique mineral product in that it is a heterogenous agglomeration of a poorly conducting rutile phase and a conducting metallic iron phase. RI and pulverized RI sintered electrodes made in this laboratory have been shown to have a very high resistance which precludes their use as electrodes. However, the carbon paste electrode technique allows the electrochemistry of both conducting and poorly conducting minerals to be investigated [4]. The reduced ilmenite carbon paste electrode (RICPE) has been used previously to study the mixed potential behaviour of the electrode in air-saturated ammonium chloride solutions as a function of rotation speed [3] and as a function of the degree of metallization of RI [5]; however the polarization behaviour of this electrode has not been investigated. In this paper, the electrochemistry of RI has been elucidated by examining its electrochemical behaviour and by making comparisons with simpler systems.

2. Experimental details

2.1. *Electrochemical techniques*

A conventional three-electrode cell was used with a platinum wire loop as the counter electrode and a 3 M KCl Ag/AgCl reference electrode, $E = 208$ mV vs SHE (standard hydrogen electrode), as the reference electrode. The electrochemical cell was similar in design to a Metrohm cell, with a basal port added to accept a luggin capillary via a Quickfit screw joint. The cell was thermostatted at 30 ± 0.1 °C. Measurements were carried out on a pure iron (99.99% Johnson Matthey) disc electrode ($r = 2.006$ mm) and carbon paste disc electrode ($r = 3.05$ mm). A Pine Model AFASRE analytical rotator was used to rotate the electrode. The rotator shaft, iron disc electrode and carbon paste holder electrode were constructed in the School of Applied Chemistry mechanical workshop at the Curtin University of Technology.

Ammonium chloride solutions were made by dissolving the solid (Univar, AR grade) in Milli-Q water (pH 4.7–4.9). Approximately 1 mM ferrous solution and hydrous ferric oxide sols [6] were made by adding appropriate amounts of solid $FeCl_2.4H_2O$ (BDH, AR grade) and $FeCl_3$ (BDH, LR grade) respectively to the above cell containing about 60 ml of deaerated electrolyte. The hydrous ferric oxide sol was clear and orange in colour. The presence of colloidal particles was confirmed by filtering through

0021-891X

a 0.22 μm membrane filter (Millipore) which removed most of the colour from the solution and left a smooth orange coloured deposit on the membrane.

The electrolyte was purged with humidified nitrogen for at least 15 min prior to immersion of the stationary or rotating electrode. A PAR model 173 potentiostat and model 175 universal programmer were used to generate polarization curves and a personal computer used to record the curves (Data Acquisition and Plotting Analysis software and A/D converter, Curtin University of Technology). All potentials are given as measured using the above reference electrode. Current densities were calculated using the geometric surface area and, for ease of comparison, all peak current densities are reported from a zero current baseline.

2.2. *Preparation of working electrodes*

The RI carbon paste was made by mixing in a 1:4 weight ratio of RI (−600 μm magnetic fraction, local industrial source) and nujol carbon paste (2:1 graphite:nujol by weight; 'ultracarbon' graphite, Ultra Carbon Corporation, Michigan USA). Preliminary tests were also conducted with 1:1 and 4:1 weight ratios using RI and pulverised RI (85% of particles between 75 and 125 μm). In addition, single grains of RI were embedded into the surface of a carbon paste electrode by simply placing the grain on the paste surface then passing a sharp steel blade over it.

Iron oxide carbon paste was prepared by mixing iron oxide and carbon paste in a 1:19 weight ratio. Hematite iron ore was used as supplied (Mano-River hematite). Oxides containing mainly lepidocrocite and magnetite (as determined by X-ray diffraction analysis) were obtained from laboratory scale Becher process aerations of RI performed at different temperatures.

Iron powder carbon paste was prepared by mixing iron powder (Koch–Light, LR) with carbon paste in the following weight ratios: 1:80, 1:15 and 1:8. Iron powder–SR carbon paste was prepared by mixing the constituents in the following weight proportions: 0.104 g iron powder, 0.296 g SR and 1.6 g carbon paste. SR from a laboraory scale Becher process aeration was leached with dilute sulfuric acid, washed and dried prior to use. The 1:15 iron powder, and iron powder–SR paste mixtures have the same weight proportion of iron as a 1:4 RI carbon paste, assuming the RI contains 26% metallic iron by weight.

The carbon paste was tightly packed into an 8–13 mm deep cavity of the carbon paste holder electrode, equipped with a screw piston. The surface was smoothed and excess material removed using a sharp steel blade. The resistance of the paste was always less than 10 Ω.

The iron disc electrode was polished on successively finer grades of SiC paper to a final grade of 2400 and then rinsed with Milli-Q water.

3. Results and discussion

In order to understand the anodic polarisation behaviour of RI, the electrochemistry of likely products from the oxidation of iron, namely ferrous and ferric ions and iron oxide, were characterized. In addition, to assess the effect of the carbon paste on the oxidation of iron and as a comparison, the electrochemistry of bulk iron and iron powder carbon paste electrodes was also considered.

3.1. *Voltammetric study of likely products from the anodic dissolution of reduced ilmenite*

3.1.1. The Fe^{2+}/Fe^{3+} couple. The electrochemical oxidation of Fe^{2+} in aqeous solution has been previously investigated in some detail (see [7] and references therein) using iron and inert metal electrodes in slightly alkaline solutions. Considering the relevance to the anodic dissolution of iron from RI, it was considered worthwhile to investigate the oxidation of Fe^{2+} in the slightly acidic conditions used in this work using a carbon paste electrode. Also, being another closely related system, a hydrous Fe(III) oxide sol in dilute ammonium chloride solution was investigated by cyclic voltammetry.

Figure 1 shows the effect of electrode rotation on the cyclic voltammogram (CV) of 1 mM Fe^{2+} in deaerated ammonium chloride solution using a carbon

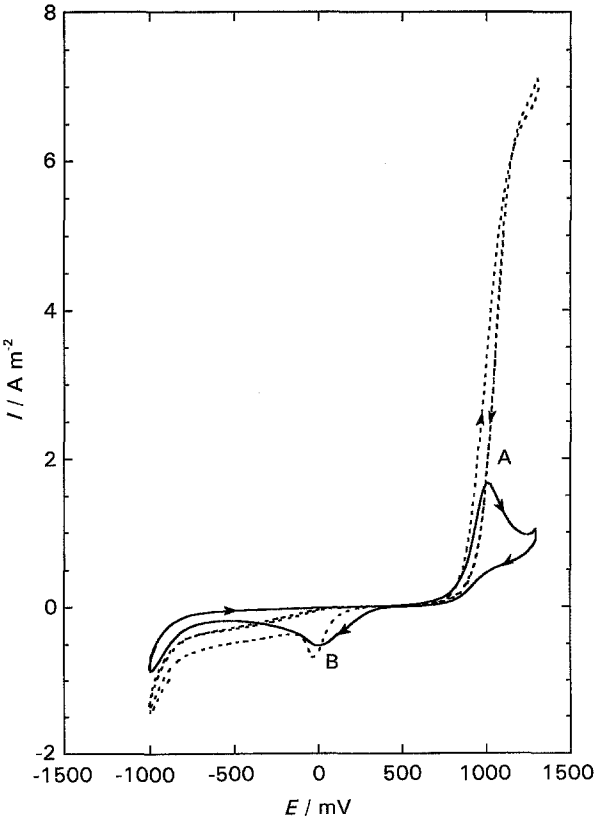

Fig. 1. Effect of electrode rotation on the CV of 1 mM $FeCl_2$ in deaerated 0.2 M NH_4Cl solution using a carbon paste disc electrode. Scan rate = 50 mV s^{-1}. First cycle only. Key: (——) 0 rpm; (- - - -) 1000 rpm.

paste disc electrode. The open circuit potential (o.c.p.) was very stable and reproducible at 0.397 V. On a stationary, fresh paste surface, if the potential sweep is initiated in the cathodic direction first, a small cathodic peak is observed at about 0 V; indicating that there may be some ferric contamination. On the reverse anodic sweep, peak A is observed at 1.010 V, corresponding to the oxidation of Fe^{2+} to Fe^{3+}. On the second cathodic sweep peak B is observed (the peak current density of B, $I_{p(B)}$, is about twice that of the peak on the first cathodic sweep), corresponding to the reduction of the Fe^{3+} produced at peak A to Fe^{2+}.

If these interpretations were completely valid then when the electrode is rotated peak B should disappear, since the Fe^{3+} produced at A will be swept away into the bulk solution. However, Fig. 1 clearly shows that peak B is still observed at 1000 rpm. This means that a solid product forms on the electrode surface at peak A. When the electrode is rotated the current at A is much larger due to the constant supply of Fe^{2+} from the bulk solution. This indicates that the solid product does not inhibit further electron transfer which means it is itself conducting and/or it does not uniformly cover the electrode, allowing electron transfer to continue on exposed sites. A similar result was obtained by Formaro [7] who investigated ferric oxide films formed by the oxidation of Fe^{2+} on a gold electrode. Also, since $I_{p(B)}$ is about the same regardless of the amount of ferric species produced at A, only a fixed amount of the solid product can adsorb onto the electrode surface (the remainder is lost to the bulk solution) or only a fixed fraction is able to be reduced at peak B.

Both peaks A and B displayed an $I_p \propto \nu^{0.5}$ and peak $E_p \propto \log \nu$ relationship which is indicative of a fully irreversible electron transfer reaction [8].

Figure 2 shows the effect of electrode rotation on the CV of a 1 mM hydrous Fe(III) oxide sol in deaerated ammonium chloride solution using a carbon paste disc electrode. If the potential is swept in the anodic direction from the o.c.p., little anodic current is observed up to the reversal potential of 1.3 V, indicating the absence of Fe^{2+}. On the return cathodic sweep peak B is observed at 0.020 V, which must correspond to the reduction of the hydrous Fe(III) oxide to Fe^{2+} which is then oxidized back to a ferric species at peak A ($E_p = 0.93$ V) on the second anodic sweep as shown. As expected, when the electrode is rotated peak A is not observed confirming that soluble Fe^{2+} is produced at peak B. Rotating disc electrode experiments revealed that the hydrous Fe(III) oxide reduction is mass transport dependent with the reduction current increasing with the electrode rotation speed. However, a plot of I_D (diffusion limited current) against $\omega^{0.5}$ shows a distinct curvature indicating that I_D is not purely diffusion controlled.

Thus from the above observations the following conclusions can be made.

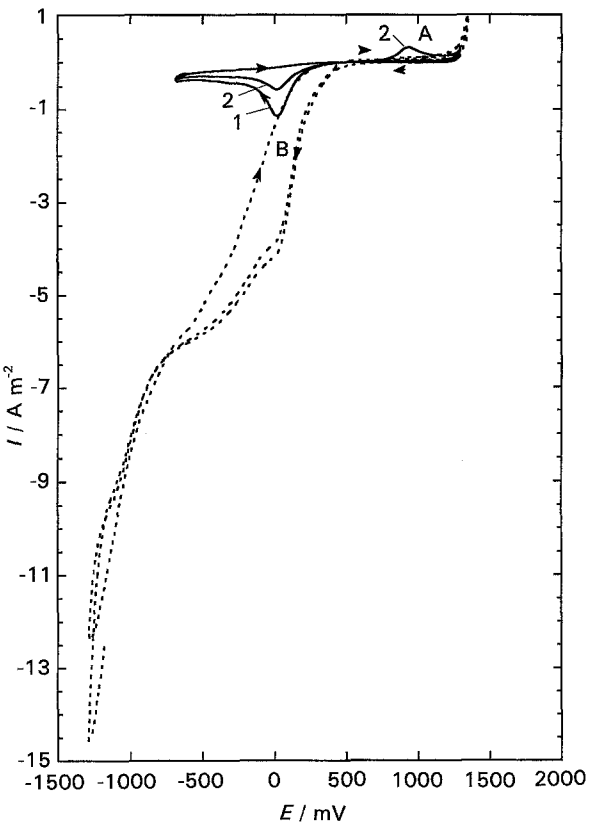

Fig. 2. Effect of electrode rotation on the CV of Fe(III) oxide sol prepared from 1 mM $FeCl_3$ in deaerated 0.2 M NH_4Cl using a carbon paste disc electrode. Scan rate 50 mV s^{-1}. Sweep initiated in anodic direction. First and second cycles as indicated. Key: (——) 0 rpm; (----) 1000 rpm.

(i) The reduction of hydrous Fe(III) oxide occurs at about 0.0 V.
(ii) Aqueous Fe^{2+} is oxidized to form hydrous Fe(III) oxide, some of which is adsorbed onto the electrode.
(iii) Adsorbed and dispersed hydrous Fe(III) oxide are reduced at the same potential.
(iv) Dispersed hydrous Fe(III) oxide is reduced to aqueous Fe^{2+}.

3.1.2. Iron oxide carbon paste electrode. The electrochemistry of iron oxide carbon paste mixtures using a conducting binder has been previously reported in the literature with the aim of developing analytical techniques for the quantitative determination of oxide stoichiometry [9–14]. The use of a conducting binder results in electron transfer occurring throughout the paste and not just at the paste/electrolyte interface. Also, acidic electrolytes used as binders resulted in chemical dissolution of the oxide within the paste. Thus the previous studies only have limited relevance to this work where a nonconducting binder was used.

The o.c.p. for hematite, lepidocrocite and magnetite carbon paste electrodes tended to drift quickly between the range of 0.10 and 0.40 V, never reaching a stable and reproducible value. This is because a defined redox couple cannot be established between the oxide and the solution, which is essentially free of Fe^{2+} and Fe^{3+} ions. For this reason most of the CVs were measured by scanning the potential in the

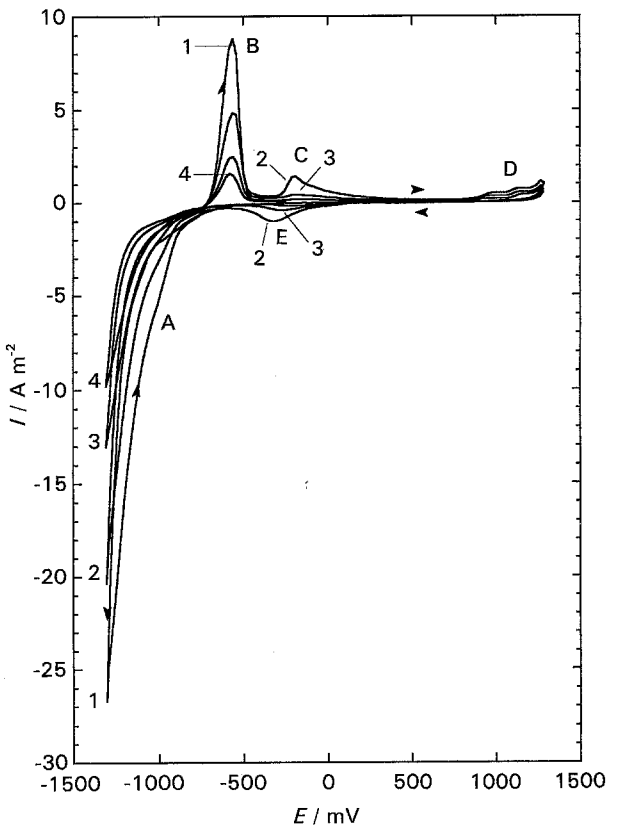

Fig. 3. Effect of multiple cycling on the CV of a 1 : 19 lepidocrocite carbon paste disc electrode in deaerated 0.2 M NH_4Cl. Stationary electrode. Scan rate 50 mV s^{-1}. Cycle number as indicated.

anodic or cathodic direction from an initial bias potential of 0 V.

Figure 3 shows the effect of multiple cycling on the CV of a lepidocrocite carbon paste electrode. CVs for hematite and magnetite carbon paste electrodes showed similar features. A cathodic reduction current A, overlapping with the hydrogen evolution reaction current, appears at about −1.0 V. For hematite, a reduction peak was resolved at −0.965 V. If the reversal potential is more negative than −1.00 V, peak B is observed on the reverse anodic scan. Peak B corresponds to the oxidation of the substance formed at A, since when the cathodic reversal potential is made more negative, peak B increases in height. The substance formed at peak A is a solid on the electrode surface since peak B is essentially unchanged when the electrode is rotated at 1000 rpm during the scan. Multiple cycling of the electrode results in a steady decrease in $I_{p(B)}$ and in the magnitude of the current at the cathodic reversal potential. This means that there is a loss of reducible oxide at the electrode surface, probably due to a simultaneous reaction involving the production of a soluble species.

The above observations are consistent with an Fe(III) oxide being reduced to a $Fe(OH)_2$ at potentials more negative than −1.00 V. For lepidocrocite, the reduction would proceed according to the following reaction [15]:

$$FeOOH(s) + H^+(aq) + e^- \rightarrow Fe(OH)_2(s) \quad (1)$$

The dissolution of $Fe(OH)_2$ is controlled by the pH near the paste/electrolyte interface and will dissolve according to the following reaction:

$$Fe(OH)_2(s) + 2H^+(aq) \rightarrow Fe^{2+}(aq) + 2H_2O \quad (2)$$

Dissolution of $Fe(OH)_2$ is slow relative to the potential sweep rate used, since peak B, corresponding to the oxidation $Fe(OH)_2$ is observed on the reverse anodic scan at −0.60 V. The slow dissolution of Fe^{2+} to the bulk solution accounts for the gradual decrease in the amount of oxide available for reduction on each successive cycle and the negligible effect that rotating the electrode has on the CV. The two small overlapping peaks, labelled D in Fig. 3, are due to the oxidation of Fe^{2+} (from the dissolution of $Fe(OH)_2$) to a Fe^{3+} species. As expected, this peak is absent when the electrode is rotated or when the potential sweep is initiated in the anodic direction on a fresh electrode. Voltammetric transitions of the iron oxides, similar to those described above are observed during the polarisation of iron electrodes in alkaline solutions [16, 17].

Peaks C and E were only observed in the CVs of magnetite and lepidocrocite carbon paste electrodes. Peak E was absent upon electrode rotation indicating the reduction of a solution species. Also, this peak is not observed on the first anodic or cathodic sweep indicating that the species being reduced was not originally in the paste and is electrochemically formed during the CV. Thus it appears that peak E corresponds to the reduction of the Fe^{3+} species formed at D. However, this potential does not correspond to the reduction of Fe(III) sol (Fig. 2), possibly due to a different level of hydration. In any case, no definite assignment of peaks C and E has been made.

3.2. *Voltammetric study of the anodic dissolution of iron in model reduced ilmenite systems*

3.2.1. Solid iron disc electrode. Figures 4 and 5 show the CV of a stationary and rotating pure iron disc electrode respectively. Scanning anodically from the o.c.p., the current increases immediately in an apparently exponential manner for the first 0.1 V and then increases in a roughly linear fashion up to 0 V; this is consistent with the formation of a partially passivating film. Above 0 V, an abrupt increase in the current, which is associated with anodic pitting, was observed, and confirmed by microscopic inspection of the electrode after the run. For the second and subsequent cycles on the same stationary electrode or if the potential is swept in the cathodic direction first on a fresh, stationary electrode, a low current density curve results and passivation is not observed (Fig. 4, cycle 2). However, when the electrode is rotated a passivation peak is observed regardless of the initial scan direction and the number of repeat potential cycles (Fig. 5).

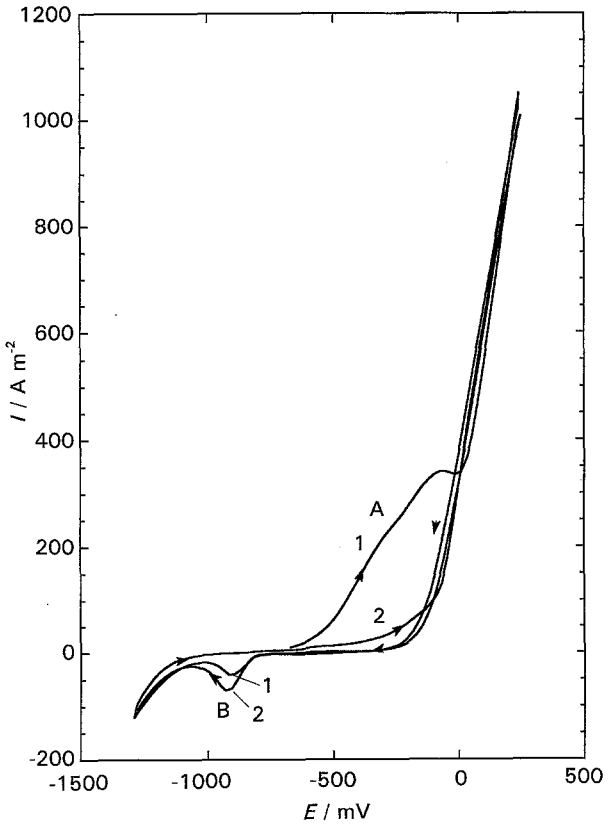

Fig. 4. The first two CV cycles of a pure iron disc electrode in deaerated 0.2 M NH_4Cl. Stationary electrode. Scan rate 50 mV s^{-1}. First and second cycles as indicated.

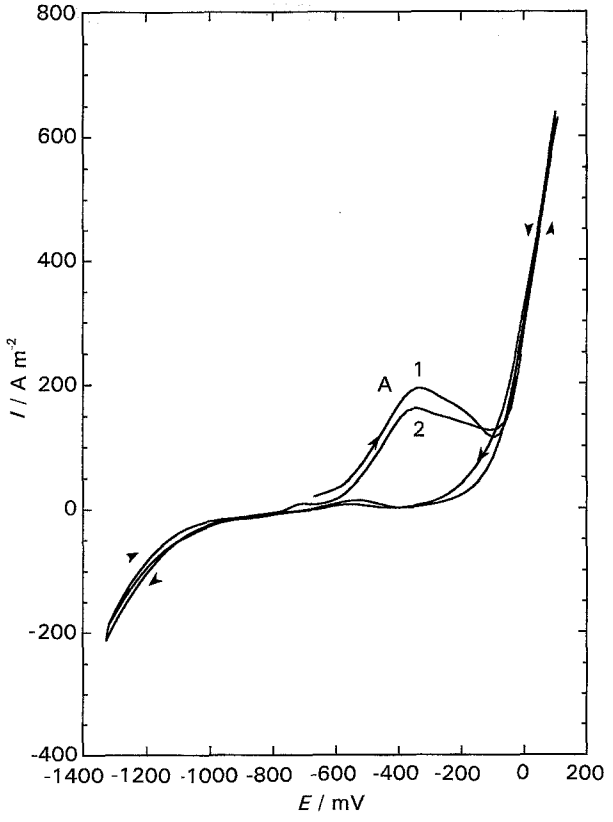

Fig. 5. The first two CV cycles of a pure iron disc electrode in deaerated 0.2 M NH_4Cl. Rotating electrode (1000 rpm). Scan rate 50 mV s^{-1}. First and second cycles as indicated.

The observations may be interpreted by considering that the dissolution reaction can be described in terms of a simplified 'hydroxide' mechanism, summarised by Sato [18] as follows:

$$Fe + H_2O \longrightarrow FeOH(ad) + H^+ + e^- \quad (3)$$

$$FeOH(ad) \longrightarrow FeOH^+(aq) + e^- \quad (4)$$

$$FeOH^+(aq) \longrightarrow Fe^{2+}(aq) + OH^- \quad (5)$$

Before polarization, the pH near the iron/electrolyte interface is the same as the bulk pH. As the potential is scanned anodically, fast active dissolution occurs according to the above mechanism, since the pH is relatively high. Eventually $Fe(OH)_2$ precipitates, passivating the iron to a small degree and limiting the dissolution rate (Fig. 4, cycle 1, 'A'). For a stationary electrode, as oxidation continues by Reactions 3 to 5, the pH at the metal/electrolyte interface decreases, eventually leading to the breakdown of the passive film (a change of dissolution mechanism [18]) and active pitting at potentials above 0 V. When the potential scan direction is reversed (on a stationary electrode) the low local pH remains, resulting in a lower dissolution current, preventing repassivation of the surface on the reverse sweep. If the potential is cycled between the o.c.p. and the anodic reversal potential a smaller anodic passivation current is observed on the second and subsequent cycles. However, if between cycles the potential is held at the o.c.p. for 22 s (the time taken to sweep from the o.c.p. to −1.3 V and back) the anodic current on the second and subsequent cycles is nearly the same as on the first cycle. This gives an idea of the amount of time required for the surface pH to increase to bulk values after the anodic scan and clearly shows that the low anodic dissolution current observed after a scan to −1.3 V is a result of another process, possibly hydrogen adsorption.

Peak B in Fig. 4 (E_p = −0.91 V) is not observed when the electrode is rotated during the CV (Fig. 5) or if the potential is swept in the cathodic direction first on a stationary fresh electrode, indicating that the peak corresponds to reduction of a solution species generated during the anodic scan. These observations are consistent with the reduction of Fe^{2+} to metallic iron at this peak. To confirm this assertion, Fe^{2+} was added to the electrolyte as $FeCl_2.4H_2O$ (~4.5 mM). A peak was then observed on the first cathodic sweep at −0.87 V (I_p = ~15 A m^{-2}) corresponding to the reduction of Fe^{2+} from the bulk solution. If the CV extends to 0.25 V, where the iron is oxidized, a single larger peak at about −0.91 V is observed on the cathodic sweep. This confirms that Fe^{2+} from the anodic dissolution of iron is reduced to metallic iron at peak B in Fig. 4.

An experimental observation not explained by the above model is the low anodic dissolution current and absence of a passivation peak when the potential is initially scanned to −1.3 V on a fresh stationary iron electrode. This means that there must be some cathodic reaction resulting in the inhibition of the

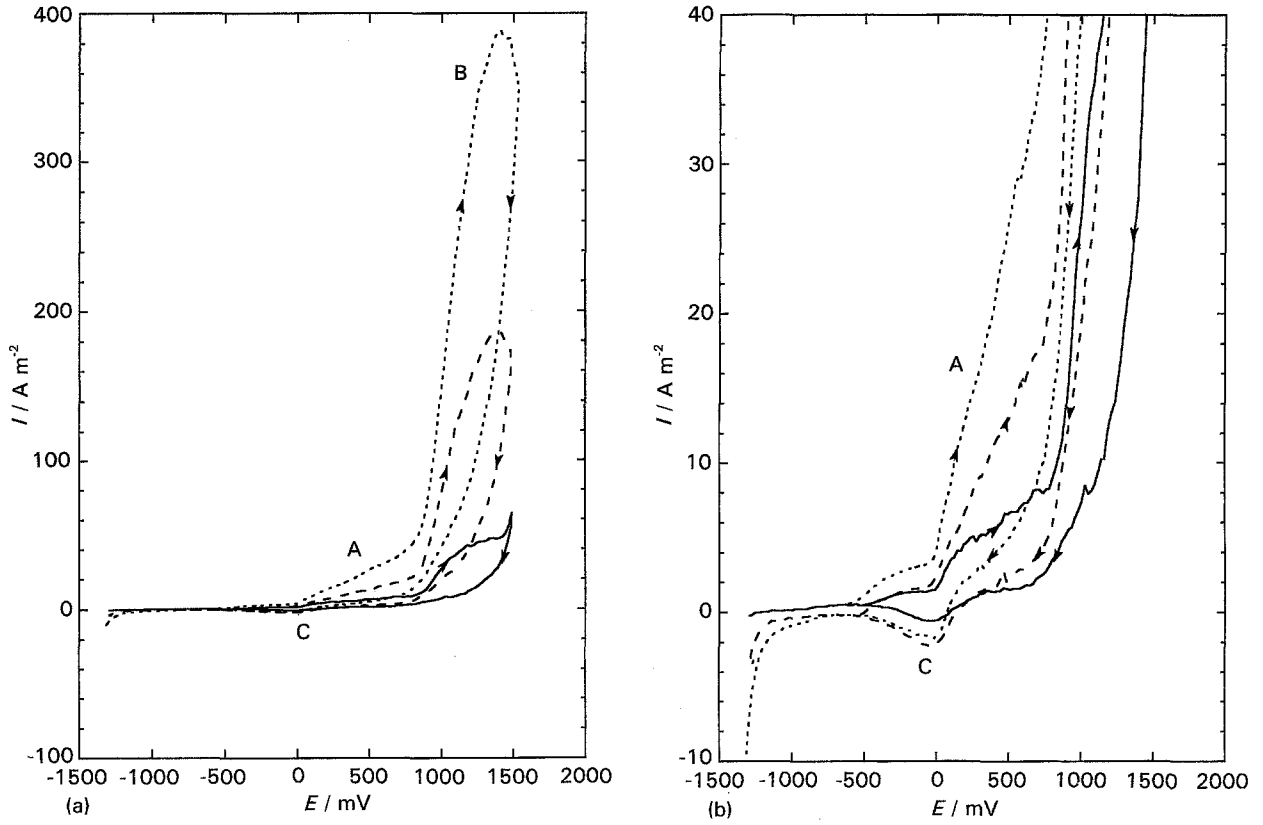

Fig. 6. (a) Effect of iron content (iron powder : carbon paste by weight) on the CV of an iron powder carbon paste electrode in deaerated 0.2 M NH_4Cl and (b) with expanded current scale. Scan rate 50 mV s^{-1}. Stationary electrode. First cycle only. Key: (——) 1 : 80; (— — —) 1 : 15; (- - - -) 1 : 8.

anodic dissolution reaction. The inhibiting effect is lost when the electrode is rotated (Fig. 5). Adsorbed hydrogen is known to inhibit the anodic dissolution of iron [19], so it seems likely that hydrogen formed at −1.3 V adsorbs on a stationary iron electrode and inhibits the anodic dissolution reaction but can be swept away into the bulk solution when the electrode is rotated.

CVs performed at 500, 1000 and 2000 rpm showed that the pitting current at 0 V is essentially independent of the electrode rotation speed. At higher rotation speeds the size of the pits decreased but their numbers increased. The pits were uniformly distributed across the electrode surface.

3.2.2. Iron powder carbon paste electrodes. Neither the Fe powder nor the RI, which is discussed in the next section, were pretreated before use. The RI is from an industrial source and like the Fe powder, was stored in air; no other special precautions were taken to prevent the formation of, or to remove, the oxide that is undoubtedly on the iron surface, prior to recording the CVs.

Figure 6(a) shows the CV of a stationary carbon paste electrode containing different weight fractions of iron powder. The o.c.p. varied between −0.52 and −0.62 V but usually an o.c.p. of about −0.58 V was observed. The o.c.p. did not show an obvious dependence upon the weight ratio of iron powder in the carbon paste; however, it is possible that some small dependence is disguised by the poor reproducibility of the o.c.p.'s. For all weight ratios, the CV showed a similar trend, with the current slowly increasing between the o.c.p. and about 0.7 to 0.8 V (Fig. 6(a), 'A'), then suddenly increasing at more anodic potentials giving rise to peak B. The anodic current density monotonously decreases on each successive cycle indicating that the iron is being removed from the paste surface. The current at 1.5 V is proportional to weight ratio of iron in the carbon paste and is independent of the electrode rotation speed. CVs of carbon paste electrodes in the absence of electroactive material showed that the background current at the anodic and cathodic limits was less than 0.7 A m^{-2} for $-1.3 < E < 1.3$, increasing to 10 A m^{-2} at 1.5 V. This indicates that iron dissolution is the predominant reaction around these potentials and the current or dissolution rate is kinetically controlled and relatively slow, since high overpotentials (E° $Fe/Fe^{2+} = -0.648$ V(Ag/AgCl), also compare with the CV for iron; see Figs 4 and 9) are required to produce a significant current.

Sweep rate experiments showed that for rates less than 50 mV s^{-1} an anodic peak was resolved at about 1.0 V. The peak current and potential decreased with decreasing sweep rate. It is believed that this peak corresponds to the build up of Fe^{2+} near the electrode surface retarding the anodic dissolution reaction. Precipitation of $Fe(OH)_2$ does not occur due to the decrease of the pH near paste/electrolyte interface resulting from the hydrolysis of Fe^{2+}. The low pH also explains the immediate and sharp decrease in the current after anodic potential reversal as discussed in Section 3.2.1.

Figure 6(b) shows the same curves as Fig. 6(a) but with the current scale expanded; revealing cathodic peak C on the reverse potential sweep at about 0.00 V. This peak is absent when the electrode is rotated at 1000 rpm indicating the reduction of a solution species. It is proposed that a small fraction of the Fe^{2+} produced at B is oxidized to Fe^{3+} which precipitates as a dispersed hydrous oxide near the paste surface. On a stationary electrode the dispersed hydrous oxide is reduced at about 0.0 V (peak C) to Fe^{2+} (see Section 3.1.1). For a rotating electrode the hydrous oxide is swept away into the bulk solution, and thus is not available for reduction on the reverse scan. Peak C showed a $I_p \propto \nu$ relationship which is generally indicative of a surface or adsorption process [8] while peak B in Fig. 2 (attributed to the reduction of adsorbed hydrous oxide) showed $I_p \propto \nu^{0.5}$ relationship. The reason for this apparent discrepancy is unclear.

Freour [14] reported CVs for iron powder carbon paste electrodes using a conducting binder in different acidic electrolytes. The CVs bear little resemblance to those shown in Fig. 6. The difference can probably be attributed to the use of a conducting binder by Freour while a nonconducting binder was used in this work.

3.2.3. Iron powder-synthetic rutile carbon paste electrode. To assess whether the TiO_2 component of RI has any effect on the anodic dissolution of iron, SR (from leached RI) was added to the iron powder carbon paste. The CV of a carbon paste containing only SR was also measured. The results of these experiments are presented below.

The o.c.p. of the stationary and rotating iron powder–SR carbon paste electrode (FeSRCPE) varied between −0.57 and −0.59 V. This indicates that the SR does not have any galvanic interactions with the Fe powder. As shown in Fig. 7, multiple cycling of the electrode does not change the general shape of the CV but the anodic current decreases monotonously on each successive cycle indicating that metallic iron is being removed from the electrode surface on each anodic sweep. Rotation of the electrode at 1000 rpm did not change the shape of the CV or the relative magnitude of the anodic current density at Peak A and B indicating that the anodic dissolution of iron is kinetically controlled.

Peak A at about −0.30 V is very close to −0.34 V observed for peak A on a pure iron rotating disc electrode (Fig. 4). Peak A was attributed to the dissolution of iron followed passivation of the iron surface by a $Fe(OH)_2$ precipitate (Section 3.2.1). It seems likely that the same process is responsible for peak A in Fig. 7.

After peak A, between 0.0 and 0.8 V, the current is essentially independent of the potential. The passive dissolution current density is very large indicating that the $Fe(OH)_2$ precipitate is not very protective.

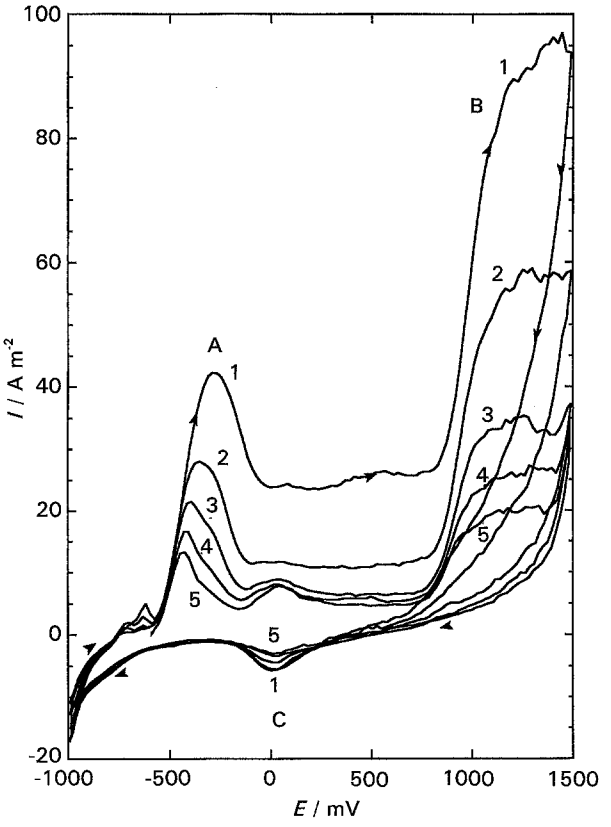

Fig. 7. Effect of multiple cycling on the CV of an iron powder–synthetic rutile carbon paste electrode (1:15 iron powder:CP; 1:5.4 SR:CP) in deaerated 0.2 M NH_4Cl. Scan rate 50 mV s^{-1}. Stationary electrode. Cycle number as indicated.

In a similar manner to the FeCPE, above 0.8 V a sudden increase in the current was observed producing peak B. For the FeSRCPE, $I_{p(B)}$ was consistently lower than for the FeCPE probably because prior dissolution at Peak A (in Fig. 7) leaves less iron available for dissolution at peak B. The strong dependence of $I_{p(B)}$ on the metallic iron content of the paste was discussed in Section 3.2.2.

Peak C occurs at about 0.01 V and can be attributed to the reduction of a hydrous Fe(III) oxide (see Section 3.1.1). The peak did not completely disappear when the electrode was rotated indicating that some adsorption may be occurring.

Since both the FeCPE and FeSRCPE contain the same proportion of iron powder, the synthetic rutile must be catalysing the anodic dissolution reaction. It was confirmed by cyclic voltammetry that synthetic rutile itself was not electrochemically active within the above potential range and therefore peak A is due solely to the anodic dissolution of iron. TiO_2; however, is known to have electrocatalytic activity. It has been shown that electrodes covered with dried TiO_2 gels enhanced the electron transfer reaction of ruthenium–ammonia complexes in phosphate buffer solutions [20] and that photolysis of water chemisorbed on TiO_2 can occur [21]. The above results show that synthetic rutile is also exerting an electrocatalytic effect on the anodic dissolution of iron.

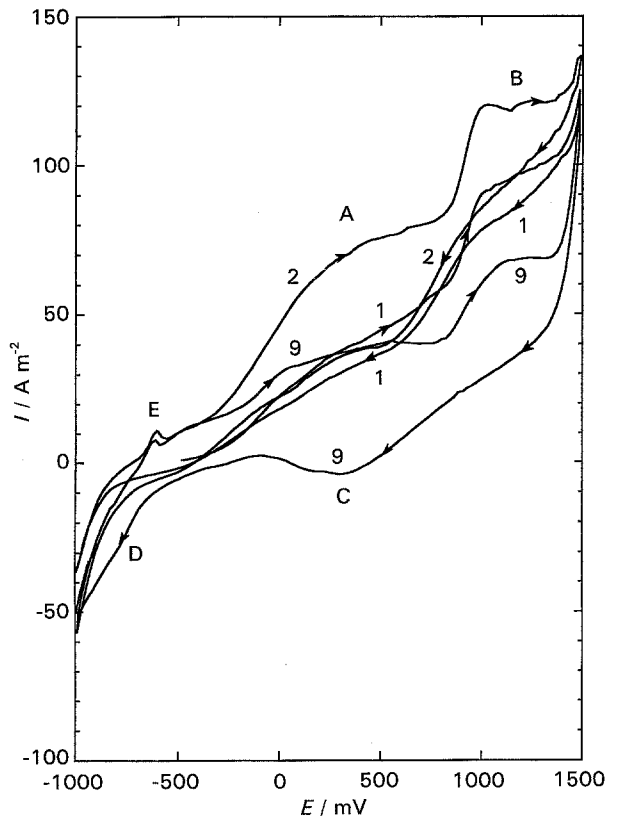

Fig. 8. Effect of multiple cycling on the CV of a 1 : 4 reduced ilmenite carbon paste electrode in deaerated 0.2 M NH_4Cl. Scan rate 50 mV s^{-1}. Stationary electrode. Cycle number as indicated.

3.3. *Voltammetric study of reduced ilmenite*

3.3.1. Reduced ilmenite carbon paste electrode. Figure 8 shows the effect of multiple cycling on the CV of a 1 : 4 reduced ilmenite carbon paste electrode (RICPE). For the first cycle the potential increases almost linearly and then increases more suddenly at about 0.8 V giving rise to peak B. A similar current increase at this potential was observed for the FeCPE and FeSRCPE in Figs 6(a) and 7, respectively. The reverse scan is almost the same as the forward scan indicating that passivation is not occurring during iron dissolution. On the second cycle the anodic dissolution current density A and B, increase. This indicates that after the first cycle the iron in RI is activated or perhaps becomes more accessible. On subsequent cycles the shape of the forward scan remains the same but the magnitude of the current decreases monotonously for each successive cycle whilst the reverse scan eventually develops a cathodic reduction peak, C, at 0.3 V. The shoulder D is due to reduction of an aged Fe(III) oxide to $Fe(OH)_2$ which is then oxidized at peak E to a Fe(III) oxide as discussed in Section 3.1.2.

Rotation of the electrode had little effect on the CV of a 1 : 4 RICPE. The independence of the anodic dissolution current density on the electrode rotation speed was confirmed by potentiostatically oxidizing the iron at 0.5 V for 3 min at various rotation speeds. It was found that the dissolution current density varied by only 1.4 A m^{-2} for rotation speeds between 0 and 2000 rpm. As expected, the dissolution current density is very strongly dependent on the potential after 3 min. For example at 0.5 and 1.4 V the current density was 7 and 12 A m^{-2}, respectively. This clearly indicates that the anodic dissolution of iron in RI is kinetically controlled.

After each of the potentiostatic polarization experiments the electrode potential was scanned in the cathodic direction at 50 mV s^{-1}. A cathodic current at about −0.9 V was observed which was not present when a cathodic scan is performed on a RICPE not subjected to anodic polarization. The cathodic peak probably corresponds to the reduction of a Fe(III) oxide (see Section 3.1.2) while a peak corresponding to the reduction of a hydrous Fe(III) oxide is not observed (Section 3.1.1).

It was found that for high anodic potentials (around 1.0 V) that the current increased in a non-linear way with increasing RI : CP (RI : carbon paste weight ratio) with significantly less current than expected for the 4 : 1 ratio. This is probably a result of dilution of the carbon paste with RI at high RI : CP ratios so that there is proportionately less carbon in contact with the iron. For this reason most of the work in this study was done using the relatively low RI : CP ratio of 1 : 4.

The CV of a pulverized 1 : 4 RICPE was similar to that described in Section 3.2.3 for the FeSRCPE where an anodic passivation peak was resolved at more negative potentials. The anodic peak occurred at about 0.0 V for the pulverized RICPE compared to −0.3 V for the FeSRCPE (Fig. 7). This result strongly suggests that the shape of the CV for the RICPE shown in Fig. 8 is characteristic of the micro environment of the iron within the RI grain. Making the iron more accessible, either by pulverizing RI or in powder form as for the FeSRCPE, results in a passivation peak at relatively negative potentials.

Figure 9 shows the first cycle CV of the various types of iron electrodes investigated in this study. The most significant difference is that passivation does not occur during the anodic polarization of RI and that the current on the reverse scan is of the same magnitude as the current on the forward scan. The FeSRCPE and FeCPE show a significant increase in the current above 0.8 V while the increase for the RICPE is not so great probably because below 0.8 V the current is much larger than for the other two. The addition of SR to make a FeSRCPE increases the dissolution rate compared to the FeCPE to such an extent that a passivation peak is observed at −0.3 V. A pure iron electrode displayed all three regimes of active dissolution, passivation and pitting dissolution at much more cathodic potentials than iron in carbon paste.

3.3.2. Individual reduced ilmenite grains embedded in the surface of a carbon paste electrode. The o.c.p. of a carbon paste electrode (CPE) in deaerated ammonium chloride solution varies between about

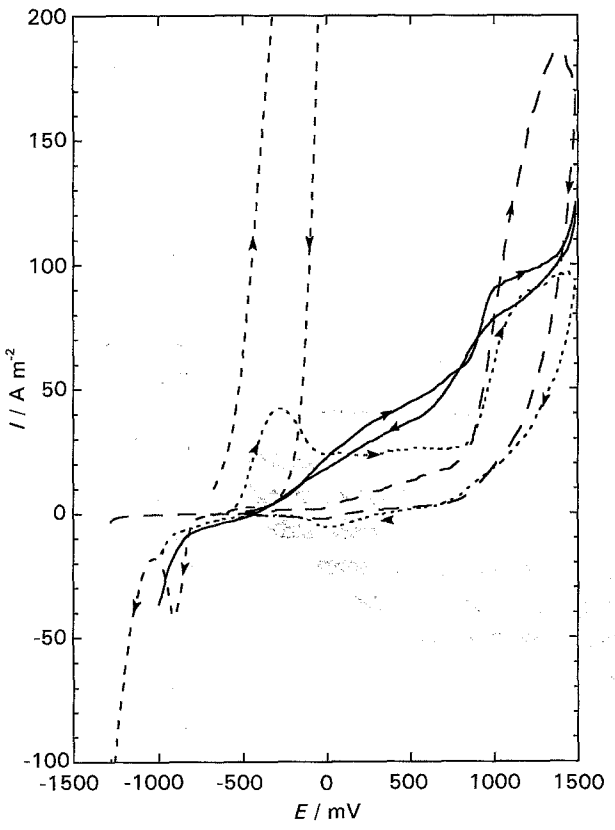

Fig. 9. CVs of iron powder–synthetic rutile (FeSRCPE), 1 : 15 iron powder (FeCPE), 1 : 4 reduced ilmenite (RICPE) carbon paste electrodes and pure iron (Fe) in deaerated 0.2 M NH_4Cl. Stationary electrode. Scan rate 50 mV s^{-1}. First cycle only. Key: (- - - -) FeSRCPE; (— —) FeCPE; (– – –) Fe; (——) RICPE.

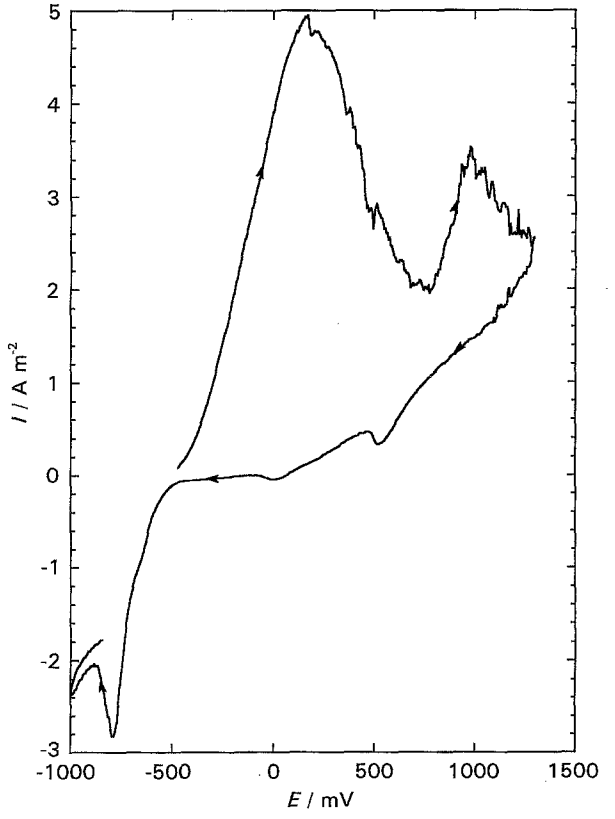

Fig. 10. CV of a single reduced ilmenite grain embedded on the surface of a carbon paste disc electrode in deaerated 0.2 M NH_4Cl. Rotating electrode (100 rpm). Scan rate 5 mV s^{-1}.

0.0 and 0.3 V. When a single RI grain is embedded into the surface, after immersion the o.c.p. very quickly stabilizes between −0.5 and −0.6 V. If the grain is dislodged (e.g., by rotating the electrode at high speeds) the o.c.p. immediately increases to that obtained on a bare CPE. This shows that the o.c.p. of the CPE with an embedded RI grain is representative of the iron and its environment within the grain.

Figures 10 and 11 show the CV of a single RI grain embedded in the surface of a rotating and stationary carbon paste electrode at sweep rates of 5 and 50 mV s^{-1} respectively. Both the current density and the general shape of the CV differed quite substantially between replicate measurements. This is not surprising considering that the current is very sensitive to changes in the iron content from grain to grain. Also, it is known that distribution of iron within reduced ilmenite is highly variable [22] and is likely to result in significant differences in the shape of the anodic polarization curves.

For CVs performed at 50 mV s^{-1} the current density increased immediately from the o.c.p. to the anodic reversal potential and then followed the same path on the cathodic sweep. This indicates that passivation was not occurring. After 6–9 cycles no peaks were observed which means that all of the available iron within the grain has been depleted. This statement is supported by the fact that the o.c.p. after multiple cycling returns to positive values.

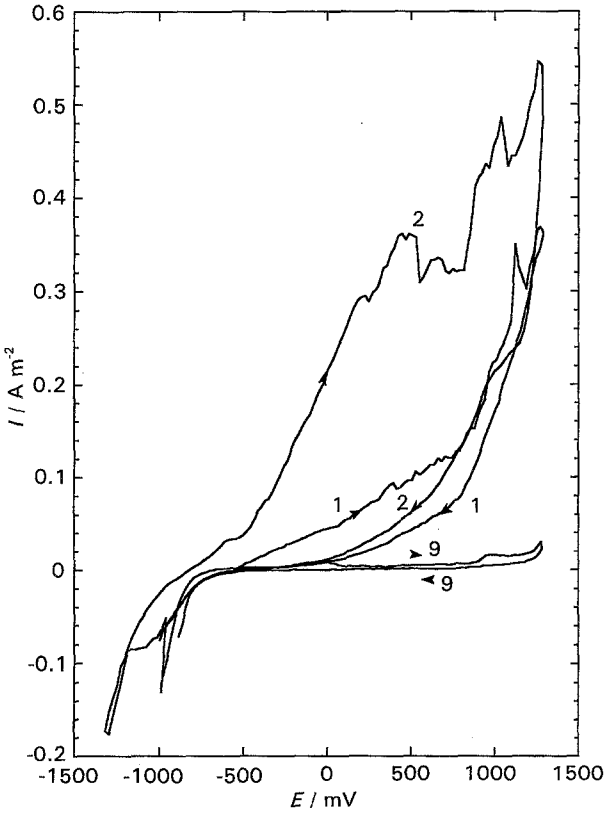

Fig. 11. Effect of multiple cycling on the CV of single reduced ilmenite grain embedded on the surface of a carbon paste disc electrode in deaerated 0.2 M NH_4Cl. Stationary electrode. Scan rate 50 mV s^{-1}. Cycle number as indicated.

At lower sweep rates (e.g., $5\,mV\,s^{-1}$ or below) it is possible to oxidize all the available iron within the first anodic potential sweep (Fig. 11).

To make further inferences about the dissolution of iron from individual ilmenite grains it may be helpful to make correlations between the iron distribution within the RI grains and polarization curves.

4. Conclusions

It was shown that in deaerated ammonium chloride solution, aqueous Fe^{2+} is oxidized to hydrous Fe(III) oxide which is then adsorbed on the electrode surface. The reduction of colloidal hydrous Fe(III) oxide occurs at about 0.0 V and is mass transport controlled to a large degree.

Pure iron displays active dissolution, followed by weak passivation prior to active pitting dissolution. The dissolution reaction can be described by the classical 'hydroxide mechanism'. The shape of the CV is strongly dependent upon the polarization history of the electrode and the solution hydrodynamics.

Three iron (III) oxides investigated displayed similar cyclic voltammetric behaviour. Iron oxide is reduced to $Fe(OH)_2$ at about -1.0 V which is then oxidized at -0.60 V.

The rate of anodic dissolution of iron powder in carbon paste is very slow. It was shown that the addition of synthetic rutile can substantially increase the rate of dissolution.

The cyclic voltammetric behaviour of RI is strongly time dependent. At low potentials the anodic dissolution reaction is not as fast as for iron powder–SR mixtures but at higher potentials the reaction is faster for iron in RI. It was shown that the anodic dissolution of iron in RI is influenced by two factors: the electrocatalytic effect of TiO_2 and the microenvironment of iron within the RI grain.

It is possible to measure the cyclic voltammogram of a single reduced ilmenite grain by embedding the grain in the surface of the carbon paste electrode.

Further work is under way to examine the relative importance of the electrocatalytic effect of TiO_2 and the microenvironment on the voltammetric behaviour of iron in reduced ilmenite.

Acknowledgements

This work was financially supported by Murdoch University, the A. J. Parker Cooperative Research Centre for Hydrometallurgy and the Minerals and Energy Research Institute of Western Australia. The authors thank the Western Australian Corrosion Facility for use of laboratory facilities, Justin Ward for supplying some of the iron oxides and Associate Professor D. Muir for helpful suggestions during the work.

References

[1] R. G. Becher, *Australian Patent 247,110* (1963).
[2] R. G. Becher, R. G. Canning, B. A. Goodheart and S. Uusna, *Proc. Aust. Inst. Min. Metall.* **21** (1965) 21.
[3] J. B. Farrow and I. M. Ritchie, *Hydrometallurgy* **18** (1987) 21.
[4] E. Ahlberg and J. Ásbjörsson, *ibid.* **34** (1993) 171.
[5] C. B. Ward, PhD thesis, Murdoch University, Western Australia, (1990).
[6] D. J. Shaw, 'Introduction to Colloid and Surface Chemistry', 4th ed., Butterworth–Heinemann, Oxford (1991).
[7] L. Formaro, *Corros. Sci.* **19** (1979) 631.
[8] A. J. Bard and L. R. Faulkner, 'Electrochemical Methods', John Wiley & Sons, New York (1980).
[9] J. M. Lecuire and Y. Pillet, *J. Electroanal. Chem.* **91** (1978) 99.
[10] Z. Z. Sharara, O. Vittori and B. Durand, *Electrochim. Acta* **29** (1984) 1689.
[11] *Idem, ibid.* **29** (1984) 1685.
[12] M. T. Mouhandess, F. Chassagneux, O. Vittori, A. Accary and R. M. Reeves, *J. Electroanal. Chem.* **181** (1984) 93.
[13] M. T. Mouhandess, F. Chassagneux and O. Vittori, *ibid.* **131** (1982) 367.
[14] R. Freour, *Electrochim. Acta* **30** (1985) 795.
[15] M. Stratmann, K. Bohnenkamp and H.-J. Engell, *Corros. Sci.* **23** (1983) 969.
[16] R. S. Schrebler Guzman, J. R. Vilche and A. J. Arvia, *Electrochim. Acta* **24** (1979) 395.
[17] H. H. Le and E. Ghali, *J. Appl. Electrochem.* **23** (1993) 72.
[18] N. Sato, *Corrosion*, **45** (1989) 354.
[19] I. Epelboin, P. Morel and H. Takenouti, *J. Electrochem. Soc.* **118** (1971) 1282.
[20] P. A. Connor, K. D. Dobson and A. J. McQuillan, 9th Australasian Electrochemistry Conference, Wollongong (1994) O17.
[21] G. N. Schrauzer and T. D. Guth, *J. Am. Chem. Soc.* **100** (1978) 7189.
[22] I. A. Grey and A. F. Reid, *The American Mineralogist* **60** (1975) 898.